PHYSICAL REVIEW B VOLUME 41, NUMBER 17 15 JUNE 1990-I

Electron band structure of a rare-earth metal: Tb(0001)

S. C. Wu,[*] H. Li, D. Tian, J. Quinn, Y. S. Li, and F. Jona
College of Engineering and Applied Science, State University of New York, Stony Brook, New York 11794-2200

J. Sokolov
Department of Physics, Queens College, City University of New York, Flushing, New York 11367-0904

N. E. Christensen
Institute of Physics, Aarhus University, DK-8000 Aarhus C, Denmark
and Max-Planck-Institut für Festkörperforschung, Postfach 80 06 65,
D-7000 Stuttgart 80, Federal Republic of Germany

(Received 16 January 1990)

The electron band structure of Tb metal has been determined at room temperature by means of angle-resolved photoemission experiments on Tb(0001). For the first time in any rare-earth metal, the full dispersed $6s$-$5d_{3z^2-1}$-type Δ_1 band has been experimentally mapped along the $\Gamma\Delta A$ line. The two critical points of the Δ_1 band have been determined at $\Gamma_1^+ = -6.9$ eV and $\Gamma_4^- = -3.6$ eV. Dispersion and width of the initial Δ_1 band are in good agreement with relativistic linear muffin-tin orbitals calculations, but the absolute energy position deviates by -1.5 eV from theory. [$\Gamma_1^+(\text{calc}) = -5.3$ eV and $\Gamma_4^-(\text{calc}) = -2.3$ eV.] The initial Δ_1 band lies well below the Fermi level, also in agreement with theory, and the experimental value of the $4f$ binding energy is about -2.6 eV.

I. INTRODUCTION

The physical and chemical properties of the rare-earth metals have long been of great scientific and technological interest, particularly because of the highly complex magnetic structures found in the pure metals and of the mixed valences assumed in several compounds.[1] These properties are intimately related to the underlying electronic structure, particularly to the fact that the $5d$-$6s$ valence states are often energetically degenerate with the shallow corelike $4f$ states. For this reason, the electron band structure of the rare-earth metals has been the object of a large number of theoretical studies ever since the mid-1960s.[2,3] Unfortunately, the results of band-structure calculations have remained essentially untested by experiment, at least in any significant quantitative detail, except for some studies of the optical density of states and of the Fermi surface by way of the de Haas–van Alphen effect[4] and positron annihilation.[5]

Although photoemission is now universally accepted as the most useful probe of the electronic structure of metals and alloys, experimental difficulties have severely limited its application to the rare-earth metals. These difficulties are primarily the preparation and the conservation of atomically clean and crystallographically ordered surfaces, and are compounded by the very small photoionizaton cross sections of the $5d$-$6s$ electrons. To date, only two reports have been published of angle-resolved photoemission measurements on rare-earth metals, one on Gd(0001) (Ref. 9) and the other on Ce{001}.[7] In Gd, a dispersing photoemission peak could be observed only for photon energies ranging between 7.5 and 10 eV (see Fig. 1 of Ref. 4), while at larger photon energies only a switch in the intensities produced by the two critical points (Γ_1^+ and Γ_4^-) could be seen. These observations are explained by a strong $k_\perp$ broadening, which is related to the exceptionally short mean free path of photoelectrons in rare-earth metals.[6]

The present paper is the first on angle-resolved photoemission measurements of a sample of Tb metal. Despite considerable experimental difficulties, particularly the unavoidable presence of large Fe impurities segregated on the (0001) surface from the bulk, we have been able to observe the full dispersed $6s$-$5d_{3z^2-1}$-type Δ_1 band along the central sixfold axis of the Brillouin zone. The energies of two critical points were measured as $\Gamma_1^+ = -6.9$ eV and $\Gamma_4^- = -3.6$ eV. The resulting experimental band structure is in good agreement with relativistic linear muffin-tin orbitals[8] (LMTO) band calculations with regard to dispersion and width of the initial Δ_1 band, but deviates from theory in the absolute energy position of the Δ_1 band by ≈ 1.5 eV [$\Gamma_1^+(\text{calc}) = -5.3$ eV and $\Gamma_4^-(\text{calc}) = -2.3$ eV, provided that eight $4f$ electrons are treated as (localized) core states]. The initial Δ_1 band lies well below the Fermi level, a result which is also consistent with the calculations. The $4f$ binding energy is found to be 2.6 eV [$4f^8 \rightarrow 4f^7(^8S_{7/2})$ ground state]. This value cannot be related to calculations which are performed within the local-density approximation (LDA).

We describe experimental details in Sec. II, present and discuss the results in Sec. III, and draw conclusions in Sec. IV.

©1990 The American Physical Society

II. EXPERIMENTAL PROCEDURES

The sample used in this work was a 2-mm-thick Tb(0001) platelet oriented, cut, and electropolished by B. J. Beaudry of the Materials Preparation Center at Ames National Laboratory. Spark-source mass-spectrometric analysis of the bulk material showed impurity levels of 59 ppm for Fe, 20 ppm for Na, 15 ppm for Cu, 10 ppm for Ca, Cl, and Gd, 5 ppm for Y, and 1 ppm or less for all other elements. The eletropolishing process of the platelet was done in a 1–6 vol % solution of perchloric acid in absolute methanol stirred and cooled to dry-ice temperatures, with a stainless-steel cathode and a current density of about 0.5 A/cm^2. This process passivates the surfaces with a chloride layer that must be eliminated by the sputtering process in ultrahigh vacuum.

The sample was wrapped in 0.05-mm-thick Ta foil, leaving a (001) surface exposed. In the experimental chamber the sample could be heated by electron bombardment of the back surface and its temperature measured by means of an infrared radiometer. The (0001) surface was cleaned, after attainment of a base pressure of about 1×10^{-10} Torr, with repeated cycles of Ar$^+$ bombardments (1×10^{-4} Torr, 400 eV, 2–3 μA) and anneals (650 °C for 10 min) with the sample either at room temperature or about 600 °C. About 50 h of Ar$^+$ bombardments were needed in order to eliminate the Cl line from the AES (Auger-electron spectroscopy) spectrum. In the process, the concentrations of N, C, and O were strongly reduced, but the Fe impurity could not be eliminated. The results presented here were obtained from "clean" surfaces characterized by the following AES peak ratios: $I(C(272\text{ eV}))/I(\text{Tb}(146\text{ eV}))$ between 0.03 and 0.07, $I(\text{O}(510\text{ eV}))/I(\text{Tb}(146\text{ eV}))$ between 0.01 and 0.03, and $I(\text{Fe}(703))/I(\text{Tb}(146\text{ eV}))$ between 0.1 and 0.2. The concentration of Fe is thereby estimated to have been between 10 and 15 at. % (see Appendix). Tests demonstrated that the segregation of Fe onto the surface of the Tb sample was promoted by the annealing process—after ion bombardment and before annealing the Tb surface was free of Fe (see Fig. 1). Since the present experiments required both "clean" and well-crystallized, and, hence, annealed, Tb surfaces, the presence of relatively high concentrations of Fe was unavoidable. Analysis of the AES data (see Appendix) shows that the iron resided almost exclusively in the first atomic layer. Fortunately, the photoemission results (see Sec. III) showed that the Fe contamination only affected the density of states near the Fermi level, with no noticeable effect on the $6s$-$5d_{3z^2-1}$-type Δ_1 band.

At the base pressure routinely reached in these experiments ($\approx1\times10^{-10}$ Torr) a "clean" Tb(0001) surface was contaminated with oxygen rather rapidly. Photoemission spectra showed that oxygen features at 5.5–6.5 eV binding energy were detectable already 15 min after a bombardment and annealing cycle, and reached an intensity comparable to that of the $6s$-$5d_{3z^2-1}$-type Δ_1 band after about 1 h (see Fig. 1). For this reason, during data collection the Tb surface was recleaned every hour with a cycle of Ar$^+$ bombardment (20 min) and annealing (650 °C for 5 min—anneals at temperatures higher than about 800 °C caused diffusion of Cl to the surface, as evidenced by the reappearance of a large Cl signal in the AES spectra).

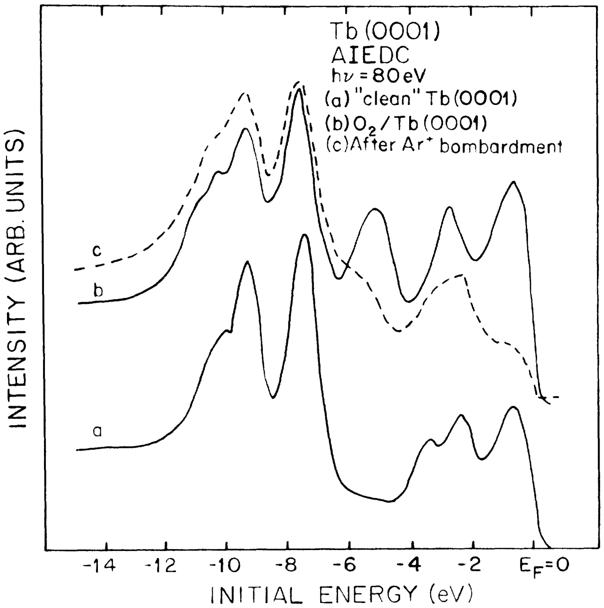

FIG. 1. Angle-integrated electron-distribution curves (EDC's) from Tb(0001) ($h\nu=80$ eV) showing the presence of Fe segregated from the bulk on the surface (peak just below E_F in curves *a* and *b*). Even at pressures of $(1-2)\times10^{-10}$ Torr the Tb surface is contaminated with oxygen within less than 1 h (peak at about -5.5 eV in curve *b*). Immediately after ion bombardment both the oxygen and the iron impurities are eliminated (curve *c*).

A "clean" Tb(0001) surface as defined above produced a low-background LEED (low-energy electron-diffraction) pattern with sharp diffraction spots. High-temperature anneals worsened the LEED pattern considerably, perhaps because of the large concentration of Cl.

The photoemission experiments were carried out at beamline U7B of the National Synchrotron Light Source in the Brookhaven National Laboratory (Upton, NY). A plane-grating monochromator was used to disperse the synchrotron light. The photoelectron energies were measured with an angle-resolved double-pass cylindrical mirror analyzer (CMA) fitted with a special slit providing an angular resolution of 2°. The sample was mounted on a manipulator that allowed rotations around three mutually perpendicular axes, so that photoemission experiments could be done with either *s*- or *s*-*p*-polarized radiation up to 25% *p*.

III. RESULTS AND DISCUSSION

Figure 2 shows normal-emission spectra from "clean" Tb(0001) taken with 25% *p*-polarized radiation and photon energies between 13 and 30 eV. We note the presence of three features in each curve, denoted *A*, *B*, and *C* in the figure, which we discuss in the following

(1) The strongest peak, *A*, located about 0.3 eV below the Fermi level, exhibits no energy dispersion in the photon-energy range shown in Fig. 2. This peak stems

from the Fe impurity on the Tb surface and disappears after Ar^+ bombardment and before anneal (see Fig. 1)—a result confirmed by resonance-photoemission experiments done with photon energies near the iron $3p$ absorption edge (not shown). Peak A has minimum intensity for $h\nu = 53$ eV (not shown here, but in agreement with the observations of Kato *et al.*[9]). The fact that there is no dispersion of peak A is consistent with the conclusion of the AES analysis (see Appendix) that most of the iron in the surface region resides in the first layer of the Tb(0001) sample.

(2) The weak peak B disperses from -6.9 eV for $h\nu = 14$ eV to -3.6 eV for $h\nu = 17.5$ eV, and then stays at -3.6 eV up to $h\nu = 30$ eV. This peak is due to direct transitions from the $6s$-$5d_{3z^2-1}$-type Δ_1 band: If the polarization of the incident radiation is changed from 25% p to pure s, peak B disappears, in accordance with the dipole selection rule for wave functions with Δ_1 symmetry. (Unfortunately, our experimental setup did not allow us to increase the p component of the exciting radiation beyond 25%, which would be expected to enhance the intensity of peak B.) Since this peak is rather weak, it may be appropriate to state that it is nevertheless a real feature, because it was observed reproducibly whenever the Tb surface was clean and ordered. Its weakness is not surprising for the following reasons. First, there is only one s-d electron in the Tb valence band. Second, the photoionization cross section of $6s$ electrons in Tb, as calculated by Yeh and Lindau,[10] is about 1 and $1\frac{1}{2}$ orders of magnitude smaller than that of $4f$ electrons. Third, owing to the exceptionally short mean free path of photoelectrons in rare-earth metals,[6] photoemission is much more surface sensitive in the rare-earths metals than in transition metals; hence, the presence of iron and of oxygen on the Tb sample swamps the Tb signal because at low photon energies the photoionization cross sections are much higher for Fe $3d$ and O $2p$ electrons than for Tb $5d$-$6s$ electrons. The fact that peak B does not disperse at photon energies larger than 18 eV is also related, we suggest, to the short mean free path and the attendant strong $k_\perp$ broadening,[6] which increases the contribution of indirect transitions at the cost of direct transitions. Hence, the signal-to-noise ratio, which arises from direct transitions, is small and the structure of the photoemission spectrum is dominated by transitions from regions of the band structure with high density of initial states (the critical points Γ_4^- and Γ_1^+). In Gd(0001) only a switch in intensity between the two critical points is seen,[6] while in the present experiments on Tb(0001) the peak corresponding to Γ_1^+ is not easily visible, possibly because of the oxygen contamination.

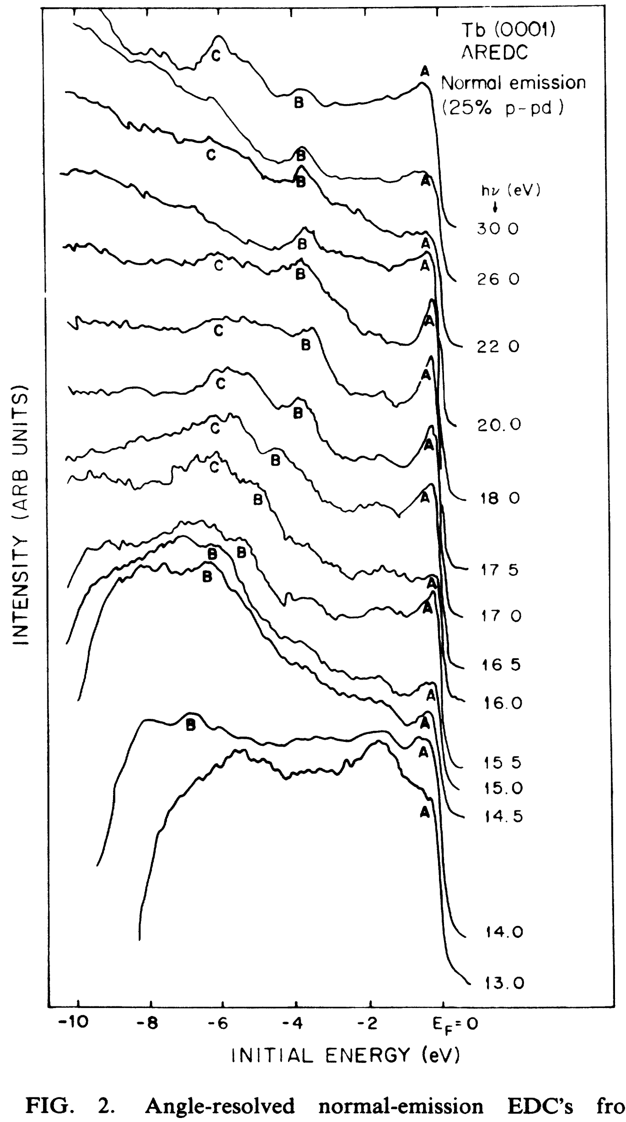

FIG. 2. Angle-resolved normal-emission EDC's from Tb(0001) for 25% p-polarized photons between 13 and 30 eV. Peaks A, B, and C are discussed in the text.

(3) Peak C, at an energy around 6 eV below the Fermi level, grew rather rapidly with time and is associated with oxygen contamination, as shown by AES scans.

Figure 3 shows two band structures of Tb, both calculated without spin polarization. The first one [Fig. 3(a)] is a straight LDA calculation, i.e., the partially filled $4f$ states are treated as self-consistently-relaxed, one-electron band states on the same footing as the rest of the conduction states. The Fermi level E_F is locked to the narrow $4f_{7/2}$ band. The total number of f electrons per atom (including a small amount, 0.06, coming from reexpansion of tails from neighbor atoms) is in this calculation 9.28, i.e., very close to an f^9 configuration. The $f_{5/2}$ band is 0.8 eV (the spin-orbit splitting) below E_F. This LDA one-electron energy is not relevant at all (see, e.g., Ref. 11) for the interpretation of the photoemission spectra that involve excitation from $4f$ states. LDA calculations can be used to yield information about the binding energy of localized states, for example, using total-energy calculations for a supercell geometry[12] to obtain the energy (Δ_-) required for the $4f^8 \rightarrow 4f^7$ excitation. Although this provides a value for Δ_- (3.1 eV, Ref. 11), the LDA theory is not about to predict a multiplet structure as is observed in photoemission data from f systems. The treatment of the $4f$ electrons as bound states also leads to calculated cohesive properties which disagree with experiments. For example, the calculated pressure at the observed equilibrium volume is -235 kbar, indicating an overly strong binding contribution from the $4f_{7/2}$ states. If, instead, we force, as in the calculation producing Fig. 3(b) eight $4f$ electrons to be localized in the core, then the theoretical equilibrium volume agrees with the experimental. As stated earlier, we cannot, in our scheme, calculate the excitation energies for the $4f$ electrons. With respect to comparison between theory and experiment for the non-f conduction states, we choose to relate to the calculation in Fig. 3(b).

Figure 4 depicts experimental bands along the $\Gamma \Delta A$ line together with the results of relativistic LMTO calculations. The initial-state energies of the principal

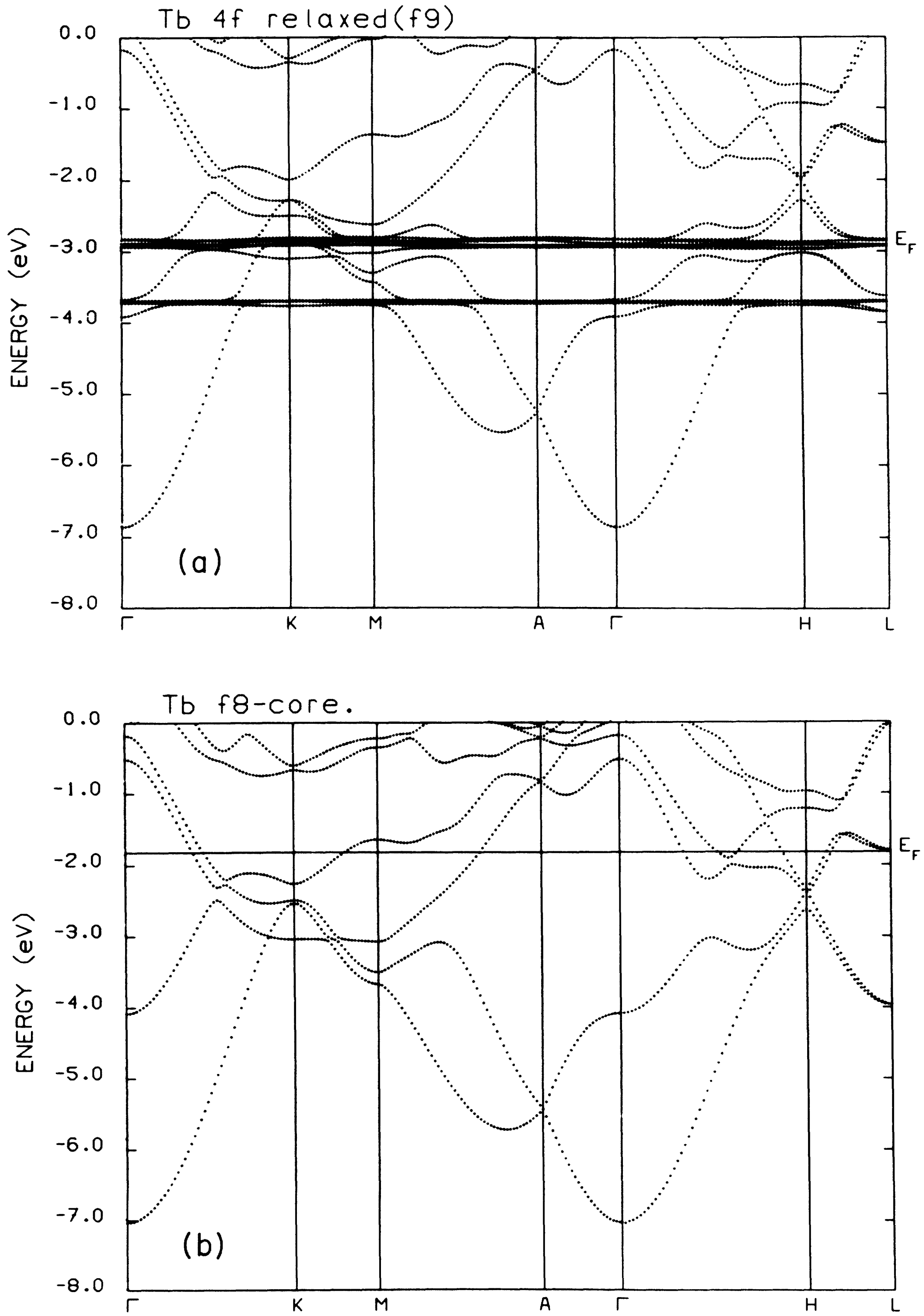

FIG. 3. (a) Band structure of Tb calculated within the LDA by means of the Dirac relativistic LMTO method. The $4f$ states are treated as relaxed band states. (b) Similar to (a), except for the fact that eight $4f$ electrons are forced to stay as ("frozen") core states (note that the free-atom configuration corresponds to $4f^9$).

transition-producing peak B range between -6.9 and -3.6 eV. We assign these two extreme energy values to the critical points Γ_1^+ and Γ_4^- of the only occupied band (in Tb there is only one $5d$ electron per atom in the valence band, and hence only one s-d-like dispersed band per atom below the Fermi level). The uncertainty in the value of Γ_1^+ is difficult to estimate, but is estimated to be larger than that of Γ_4^- (± 0.15 eV) because the maximum in the binding energy of peak B may occur for somewhat lower photon energy than 14 eV (Fig. 2). Both the width and dispersion of the occupied band are consistent with the present calculations and those of Jackson.[13] The symmetry character of the two critical points is s-d_{3z^2-1}, in accordance with Freeman's labels in the band-structure calculations of rare-earth metals.[3] The limiting values of the initial-state energies given by peak B, at $h\nu = 14$ and 17.5 eV, locate the Γ points of the final-state bands at 7.1 and 13.9 eV, respectively.

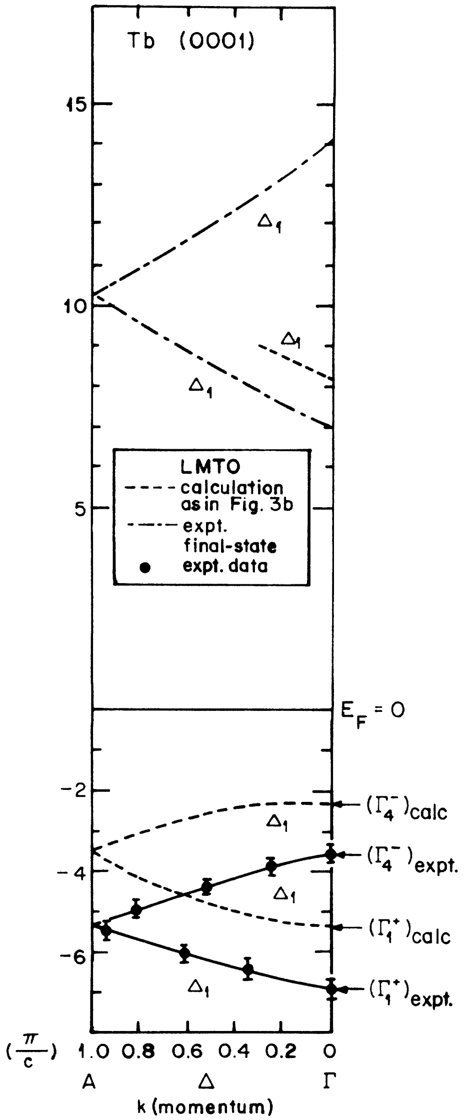

FIG. 4. Electron band structure of Tb along the $\Gamma\Delta A$ line. The experimental Δ_1 band lies lower than theory by about 1.5 eV, although dispersion and width are in good agreement with the calculations.

In order to map out the initial band from the experimental photoemission data, we must know the precise structure of the final-state bands. The revies of rare-earth band structures, by Liu,[2] by Dimmock,[14] and by Harmon,[15] are in accordance with one another in indicating that the bands are not free-electron-like but have substantial d character. According to the present calculations, the final-state band along $\Gamma\Delta A$, which starts at Γ_4^- about 10 eV above the Fermi level, is the only energetically accessible final-state band in the experiment (Fig. 4). The calculations show that the s, d, and f components of the wave function at this Γ_4^- point (10 eV above the Fermi level) are 52%, 43%, and 5%, respectively. The interaction between the final $6s$-$5d_{3z^2-1}$-type Δ_1 band and the unoccupied $4f$ band, which is located between 2 and 6 eV above the Fermi level,[16] will make the dispersion of the final Δ_1 band markedly smaller than that of a free-electron band. Thus, the final band for direct transitions that we have adopted in this work was obtained from a band in the effective-mass approximation fitted to experimentally verified calculated critical points. The procedure followed in order to determine this band was the following. The values of the final-state energies 7.1 and 13.9 eV at the Γ points $k_\perp = 2\Gamma A$ and $4\Gamma A$, respectively, were used to fit the final band in the range $2\Gamma A \leq k_\perp \leq 4\Gamma A$ to the simple (parabolic) form

$$E_f - |V_0| = \frac{\hbar^2}{2m_e^*} k_f^2 , \tag{1}$$

where E_f is the final-state energy, V_0 the inner potential, m_e^* the effective mass, and k_f the magnitude of the final-state wave vector. Thus, we find that the effective mass m_e^* is about $2m_e$ (m_e is the free-electron mass) and the inner potential V_0 is -4.8 eV. The final band used in this work is shown as a dashed-dotted line in Fig. 4.

The experimental band structure is shown with solid circles (solid line) in Fig. 4. The agreement with the calculation is good with regard to width and dispersion of the initial Δ_1 band, although the absolute energy position deviates by 1.5 eV from the present straight LDA calculation [Fig. 3(b)] and by 1.8 eV from that of Jackson.[13]

Since the ionization cross section of $4f$ electrons is very low for photon energies $h\nu$ smaller than 30 eV (Ref. 10), no features due to $4f$ electrons are visible in Fig. 2. To study the $4f$ states, we monitored angle-integrated photoemission spectra in the photon-energy range between 80 and 165 eV (see Fig. 5). The spectrum taken with $h\nu = 80$ eV is very similar to that published by Gerken *et al.*,[17] except for a much higher density of states at the Fermi level in our curve, which is due to the unavoidable presence of iron. The peaks located at -2.6, -7.7, -9.5, and -10.4 eV are due to $4f$ electrons.[16] The peak at -3.6 eV merits further discussion.

Gerken *et al.*[17] suggest that this peak is due to the surface core-level shift of $4f$ electrons in the first atomic layer, because no peak in this energy range is found in x-ray photoemission-spectroscopy (XPS) spectra, but our resonance-photoemission data indicate that this peak has an origin different from the $4f$ electrons. Figure 6 shows that near the Tb $4d$ absorption edge (150–153 eV) the -3.6-eV peak exhibits different resonance behavior from the -2.6-eV peak, and hence these two peaks cannot originate from the same $4f$ level. Absorption spectra confirm this conclusion: Fig. 6 depicts the absorption spectrum of Tb in the region of the Tb $4d$ edges as measured on our Tb(0001) sample by monitoring the integrated current of secondary electrons in the kinetic-energy range from 0 to 5 eV. There are two absorption peaks in this energy range, a small one at $h\nu=144$ eV and a large one at $h\nu=153$ eV, in good agreement with the result obtained by Allen *et al.*[18] from $TbCo_2$. The photoemission spectra in Fig. 5 show that the -3.6-eV peak has a resonance at slightly lower photon energy than the -2.6-eV peak. This kind of phenomena has been observed in the rare-earth compounds $CeSi_2$ and LaB_6,[20] and was predicted theoretically by Zangwill and Soven:[21] the states with principal quantum number $n=5$ are expected to resonate at slightly lower photon energy than the states with quantum number $n=4$. We know from XPS measurements that the -2.6-eV peak originates from the $4f$ electrons, and from our band mapping that the -3.6-eV peak corresponds to the Γ_4^- critical point of the initial state. The present calculations indicate that the s, d, and f components of the wave function at this Γ_4^- point (3.6 eV below the Fermi level) are 30%, 54%, and 16%, respectively. This Γ_4^- point has the highest density of states and the largest d component among the other states in the initial Δ_1 band. Thus, resonance photoemission data reveal that the -3.6-eV peak does not originate from the $4f$ electrons in the first layer, but rather from the $5d$ electrons. The reason that this peak disappears from XPS spectra is that the photoionization cross section of the $5d$ electrons is very small at XPS energies.

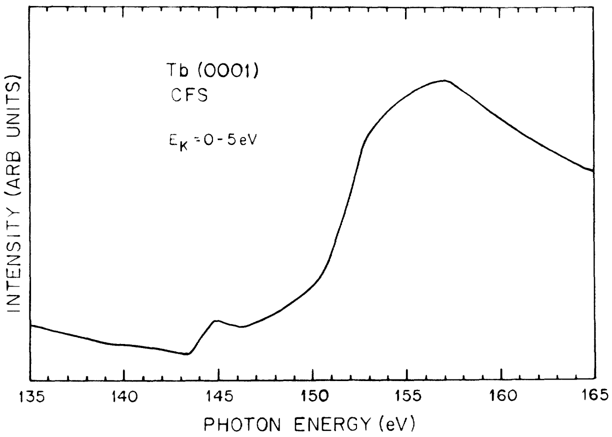

FIG. 6. Absorption spectrum of Tb in the energy range of the $4d$ edges (constant final state).

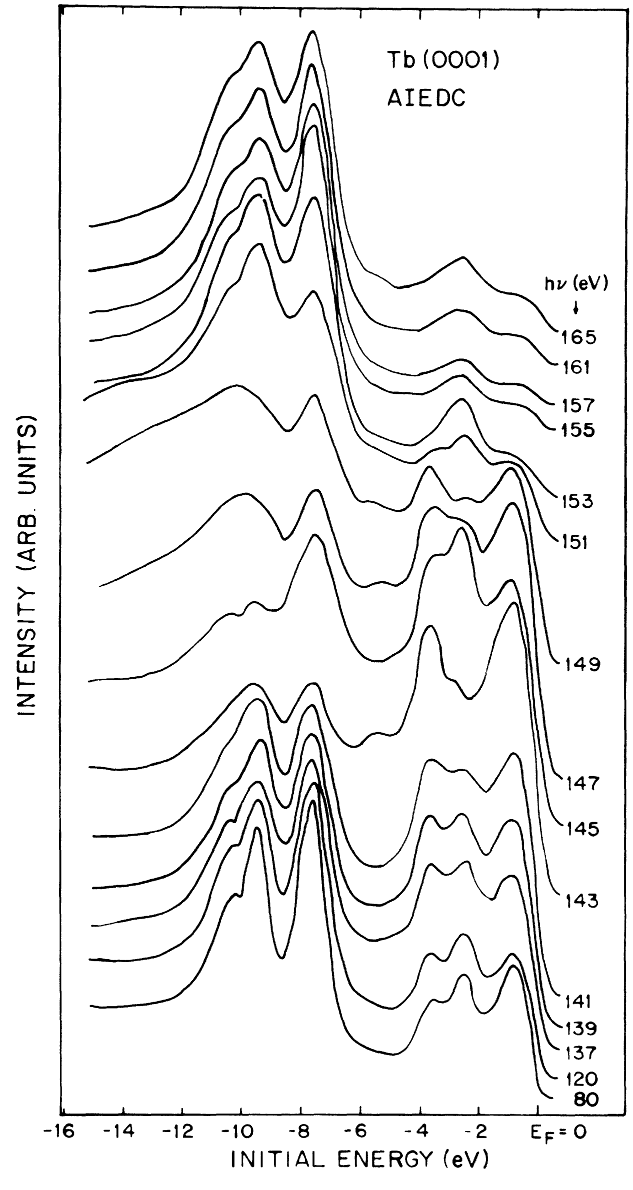

FIG. 5. Angle-integrated EDC's from Tb(0001) for photon energies between 80 and 165 eV.

IV. CONCLUSIONS

Angle-resolved photoemission experiments have been carried out on Tb(0001) in the photon-energy range 13–30 eV. Despite the presence of Fe on the surface in concentrations of 10–15 at. %, the valence-band structure was determined along the high-symmetry $\Gamma\Delta A$ line, revealing the full dispersion of the $6s$-$5d_{3z^2-1}$-type Δ_1 band for the first time in any rare-earth metal. The critical points for this Δ_1 band were determined to be $\Gamma_1^+=-6.9$ eV and $\Gamma_4^-=-3.6$ eV. Dispersion and width of the initial Δ_1 band are in good agreement with relativistic LMTO band calculations, but absolute energy positions deviate from theory by 1.5 eV. The reasons for this large discrepancy in energy position are not fully clear at this time. Obviously, the calculations neglect effects which may be very important, namely those related to the magnetic properties of Tb. These will be examined in a calculation which includes spin polarization of the conduction electrons, and where the $4f$ orbital plus spin moment has been frozen in to the experimental value. Since this is very large in magnitude, sizable shifts of the conduction bands, as compared to those derived without polarization, may be expected.

Resonance photoemission around the Tb $4d$ absorption edges shows that a peak observed at -3.6 eV in the photoemission spectra does not originate from the surface core-level shift of $4f$ electrons in the first layer, but rather from $5d$ electrons near the critical point Γ_4^- of the initial Δ_1 band, in accordance with the present band-mapping results.

ACKNOWLEDGMENTS

We acknowledge partial support of this work by the U.S. Department of Energy with Grant No. DE-FG02-86ER45239. One of us (S.C.W.) is also indebted to the Science and Technology Commission of the People's Republic of China for partial support through Grant No. 9187002.

APPENDIX

From the reference book of standard AES data[22] we calculate that the ratio of the intensity I_{Fe} (703 eV) of the Fe AES peak at 703 eV to the intensity I_{Fe} (47 eV) of the Fe AES peak at 47 eV is 0.63. From the formula[23]

$$\lambda=\frac{1430}{e^2}+0.54\sqrt{E}\ ,$$

we calculate the mean free path λ of the corresponding Auger electrons as $\lambda_{\mathrm{Fe}\,(703\,\mathrm{eV})}=14.3$ Å and $\lambda_{\mathrm{Fe}\,(47\,\mathrm{eV})}=4.35$ Å. The intensity of an AES peak is given by the formula

$$I=S\int_0^\infty N(z)e^{-z/\lambda}dz\ ,$$

where S is a sensitivity factor that depends on the Auger-electron excitation cross section and $N(z)$ is the atomic density of iron at level z. Hence,

$$\frac{I_{\mathrm{Fe}\,(703\,\mathrm{eV})}}{I_{\mathrm{Fe}\,(47\,\mathrm{eV})}}=\frac{S_{\mathrm{Fe}\,(703\,\mathrm{eV})}\int_0^\infty N(z)e^{-z/\lambda_{\mathrm{Fe}\,(703\,\mathrm{eV})}}dz}{S_{\mathrm{Fe}(47\,\mathrm{eV})}\int_0^\infty N(z)e^{-z/\lambda_{\mathrm{Fe}\,(47\,\mathrm{eV})}}dz}\ .$$

For pure iron, $N(z)$ is independent of z, so that $\int_0^\infty N(z)\exp(-z/\lambda)dz=N\int_0^\infty\exp(-z/\lambda)dz=N\lambda$, and therefore

$$\frac{I_{\mathrm{Fe}(703\,\mathrm{eV})}}{I_{\mathrm{Fe}\,(47\,\mathrm{eV})}}=\frac{S_{\mathrm{Fe}\,(703\,\mathrm{eV})}}{S_{\mathrm{Fe}\,(47\,\mathrm{eV})}}\frac{14.3\ \text{Å}}{4.35\ \text{Å}}\ ,$$

whence, since $I_{\mathrm{Fe}\,(703\,\mathrm{eV})}/I_{\mathrm{Fe}(47\,\mathrm{eV})}=0.63$,

$$\frac{S_{\mathrm{Fe}\,(703\,\mathrm{eV})}}{S_{\mathrm{Fe}\,(47\,\mathrm{eV})}}=0.192\ .$$

If all Fe atoms were located in the first layer of the Tb(0001) surface, then the relative intensities of the two Fe AES lines would be

$$\frac{I_{\mathrm{Fe}\,(703\,\mathrm{eV})}}{I_{\mathrm{Fe}\,(47\,\mathrm{eV})}}=\frac{S_{\mathrm{Fe}\,(703\,\mathrm{eV})}}{S_{\mathrm{Fe}\,(47\,\mathrm{eV})}}=0.192\ .$$

If all Fe atoms were located in the second layer, then

$$\frac{I_{\mathrm{Fe}\,(703\,\mathrm{eV})}}{I_{\mathrm{Fe}\,(47\,\mathrm{eV})}}=\frac{S_{\mathrm{Fe}\,(703\,\mathrm{eV})}}{S_{\mathrm{Fe}\,(47\,\mathrm{eV})}}\frac{e^{-d_0/\lambda_{\mathrm{Fe}\,(703\,\mathrm{eV})}}}{e^{-d_0/\lambda_{\mathrm{Fe}\,(47\,\mathrm{eV})}}}$$

$$=0.302\ ,$$

where we have chosen $d_0=2.85$ Å and have assumed that the mean free path of Fe Auger electrons in Tb is the same as in Fe. If all Fe atoms reside in the third layer, then we find $I_{\mathrm{Fe}\,(703\,\mathrm{eV})}/I_{\mathrm{Fe}(47\,\mathrm{eV})}=0.477$.

Experimentally, after overnight sputtering of the Tb(0001) surface at a pressure of 1×10^{-4} Torr of Ar with the sample at about 500 °C, and a successive anneal at 650 °C for 10 min, we measure from the AES spectrum that $I_{\mathrm{Fe}\,(703\mathrm{eV})}/I_{\mathrm{Fe}\,(47\,\mathrm{eV})}=0.18$, from which we conclude that most of the Fe atoms reside, in fact, in the first layer of the Tb sample.

---

*On leave from the Department of Physics, Peking University, Beijing 100 871, The People's Republic of China.

[1] F. P. Netzer and J.A.D. Matthew, Rep. Prog. Phys. **49**, 621 (1986).

[2] S. H. Liu, in *Handbook on the Physics and Chemistry of Rare-Earth Metals,* edited by K. A. Gschneidner, Jr. and L. R. Eyring (North-Holland, Amsterdam, 1978), Vol. 1, p. 233.

[3] A. J. Freeman, in *Magnetic Properties of Rare-Earth Metals,* edited by R. J. Elliott (Plenum, London, 1972), Chap. 6.

[4] S. Tanuma *et al.*, Phys. Lett. **25A**, 669 (1967); Solid State Commun. **8**, 1107 (1970).

[5] R. W. Williams, T. L. Loucks, and A. R. Mackintosh, Phys. Rev. Lett. **16**, 168 (1966); R. W. Williams and A. R. Mackintosh, Phys. Rev. **168**, B679 (1969).

[6] F. J. Himpsel and B. Reihl, Phys. Rev. B **28**, 574 (1983).

[7] G. Rosina, E. Bertal, F. P. Netzer, and J. Redinger, Phys. Rev. B **33**, 2364 (1986).

[8] O. K. Andersen, Phys. Rev. B **12**, 3060 (1975); N. E. Christensen, Int. J. Quantum Chem. **25**, 233 (1984).

[9] H. Kato, T. Ishii, S. Masuda, Y. Harada, T. Miyano, T. Komeda, M. Onchi, and Y. Sakisaka, Phys. Rev. B **32**, 1992 (1985).

[10] J. J. Yeh and I. Lindau, At. Data Nucl. Data Tables **32**, 1 (1985).

[11] J. F. Herbst and J. W. Wilkins, in *Handbook on the Physics and Chemistry of Rare Earths,* edited by K. A. Gschneidner, Jr., L. Eyring, and S. Hüfner (Elsevier, Amsterdam, 1987), Vol. 10, p. 321.

[12] A. J. Freeman, B. I. Min, and M. R. Norman, in *Handbook on the Physics and Chemistry of Rare Earths,* edited by K. A. Gschneidner, Jr., L. Eyring, and S. Hüfner (Elsevier, Amsterdam, 1987), Vol. 10, p. 165.

[13] C. Jackson, Phys. Rev. B **178**, 947 (1969).

[14] J. O. Dimmock, in *Solid State Physics,* edited by H. F. Ehrenreich, F. Seitz, and D. Turnbull (Academic, New York, 1971), Vol. 26, p. 104.

[15] B. N. Harmon, J. Phys. (Paris) Colloq. **40**, C5-65 (1979).

[16] J. K. Lang, Y. Baer, and P. A. Cox, J. Phys. F **11**, 121 (1981).

[17] F. Gerken, A. S. Flodström, J. Barth, L. I. Johansson, and C.

Kunz, Phys. Scr. **32**, 43 (1985).

[18] J. W. Allen, S. J. Oh, I. Lindau, and L. I. Johansson, Phys. Rev. B **29**, 5927 (1984).

[19] J. M. Lawrence, J. W. Allen, S. J. Oh, and I. Lindau, Phys. Rev. B **26**, 2362 (1982).

[20] M. Aono, T. C. Chaing, F. J. Himpsel, and D. E. Eastman, Solid State Commun. **37**, 471 (1981).

[21] A. Zangwill and P. Soven, Phys. Rev. Lett. **45**, 204 (1980).

[22] L. E. Davis, N. C. MacDonald, P. W. Palmberg, G. E. Riach, and R. E. Weber, *Handbook of Auger Electron Spectroscopy* (Physical Electronic Industries, Inc., Eden Prairie, MN, 1978).

[23] M. P. Seah and W. A. Dench, Surf. Interface Anal. **1**, 2 (1979), formula (5) and Table 1.